Relaxing the Nicotinamide Cofactor Specificity of Phosphite Dehydrogenase by Rational Design[†]

Ryan Woodyer,[‡] Wilfred A. van der Donk,*[,‡] and Huimin Zhao*[,§]

Departments of Chemistry and Chemical and Biomolecular Engineering, University of Illinois at Urbana−Champaign, 600 South Mathews Avenue, Urbana, Illinois 61801

Received June 13, 2003; Revised Manuscript Received August 11, 2003

ABSTRACT: Homology modeling was used to identify two particular residues, Glu175 and Ala176, in *Pseudomonas stutzeri* phosphite dehydrogenase (PTDH) as the principal determinants of nicotinamide cofactor (NAD^+ and $NADP^+$) specificity. Replacement of these two residues by site-directed mutagenesis with Ala175 and Arg176 both separately and in combination resulted in PTDH mutants with relaxed cofactor specificity. All three mutants exhibited significantly better catalytic efficiency for both cofactors, with the best kinetic parameters displayed by the double mutant, which had a 3.6-fold higher catalytic efficiency for NAD^+ and a 1000-fold higher efficiency for $NADP^+$. The cofactor specificity was changed from 100-fold in favor of NAD^+ for the wild-type enzyme to 3-fold in favor of $NADP^+$ for the double mutant. Isoelectric focusing of the proteins in a nondenaturing gel showed that the replacement with more basic residues indeed changed the effective p*I* of the protein. HPLC analysis of the enzymatic products of the double mutant verified that the reaction proceeded to completion using either substrate and produced only the corresponding reduced cofactor and phosphate. Thermal inactivation studies showed that the double mutant was protected from thermal inactivation by both cofactors, while the wild-type enzyme was protected by only NAD^+. The combined results provide clear evidence that Glu175 and Ala176 are both critical for nicotinamide cofactor specificity. The rationally designed double mutant might be useful for the development of an efficient in vitro NAD(P)H regeneration system for reductive biocatalysis.

Driven by recent technical advances in genetic engineering and new societal needs, the use of enzymes and microorganisms as catalysts to synthesize chemicals and materials is rapidly expanding (*1*−*5*). However, many challenges have yet to be fully addressed, such as the developmental costs of biocatalysts and the type of chemistry performed. Most biocatalysts currently used in industry (∼65%) are hydrolases (*6*) that do not perform complex chemistry. The primary reason for the low usage of enzymes catalyzing complicated chemical reactions is that such enzymes often require one or more costly cofactors, making them industrially impractical when the cofactor is added in a stoichiometric amount.

Oxidoreductases, for example, can be used for synthesis of chiral compounds, complex carbohydrates, and isotopically labeled compounds, but they often require NADH[1] or NADPH as cofactors. The cost of NADH is $40/mmol, while the price of NADPH is nearly $500/mmol (Sigma 2002 catalog), rendering stoichiometric use of either reduced cofactor at the kilogram scale prohibitively expensive. Various laboratories have thus been interested in developing regeneration systems for NAD(P)(H) that would allow their addition in catalytic amounts, with the goal of making redox bioprocesses industrially feasible. Since approximately 80% of all reductases utilize NAD(P)(H) as a cofactor accounting for over 300 known reactions (*7*), regeneration of these cofactors would be particularly advantageous.

A number of enzymatic, electrochemical, chemical, photochemical, and biological methods have been developed to regenerate cofactors (*8*−*10*). Advantages of cofactor regeneration besides reduced cost include simplified reaction workup, prevention of product inhibition by the cofactor, and sometimes a favorable influence on the reaction equilibrium (*9*). In some uses, the regenerative system drives the synthetic reaction forward even when the formation of the desired product is less favored under standard conditions. Specific advantages of enzymatic strategies include high selectivity, compatibility with synthetic enzymes, and high turnover numbers in certain cases (*9*). Criteria considered for effective enzymatic methods include the expense and stability of the enzyme, cost of the substrate for the regenerative enzyme, ease of product purification, catalytic

[†] Support for this research was provided by the Biotechnology Research and Development Consortium (BRDC) (Project 2-4-121).

* To whom correspondence should be addressed. W.A.V.: phone, (217) 244-5360; fax, (217) 244-8024; e-mail, vddonk@uiuc.edu. H.Z.: phone, (217) 333-2631; fax, (217) 333-5052; e-mail, zhao5@uiuc.edu.

[‡] Department of Chemistry, University of Illinois at Urbana−Champaign.

[§] Department of Chemical and Biomolecular Engineering, University of Illinois at Urbana−Champaign.

[1] Abbreviations: CANS, Computer Application and Network Services; DH, dehydrogenases; FPLC, fast-performance liquid chromatography; HPLC, high-performance liquid chromatography; IEF, isoelectric focusing; IPTG, isopropyl β-D-thiogalactopyranoside; MOE, molecular operating environment; NAD^+ and NADH, nicotinamide adenine dinucleotide; $NADP^+$ and NADPH, nicotinamide adenine dinucleotide phosphate; NBT, nitro blue tetrazolium; NMR, nuclear magnetic resonance; PMS, phenazine methosulfate; Pt-H, phosphite; PTDH, phosphite dehydrogenase; PCR, polymerase chain reaction; PDB, Protein Data Bank; RMS, root mean square; WT, wild type.

10.1021/bi035018b CCC: $25.00
Published on Web 09/17/2003

efficiency, K_M for the cofactor, and thermodynamic driving force of the regenerative enzyme.

Of the enzymatic NADH regeneration systems, the best and most widely used enzyme is formate dehydrogenase (FDH) from *Candida boidinii* (*11*, *12*). The recently discovered phosphite dehydrogenase (PTDH) from *Pseudomonas stutzeri* (*13*) may have kinetic and practical advantages over FDH in certain applications. A recent report highlights the benefits of using PTDH as a regeneration system (*14*). This enzyme catalyzes the nearly irreversible oxidation of hydrogen phosphonate (phosphite) to phosphate with the concomitant reduction of NAD^+ to NADH. The large change in free energy of this reaction ($\Delta G^{\circ\prime} = -63.3$ kJ/mol estimated from redox potentials) and the associated high equilibrium constant ($K_{eq} = 1 \times 10^{11}$) makes PTDH a promising NADH regenerative enzyme (*14*). A particularly interesting application of PTDH is the facile production of isotopically labeled products. Deuterium- or tritium-labeled water can be used to readily and economically prepare labeled phosphite (*15*). Subsequent use of isotopically labeled phosphite during a synthetic reduction using PTDH for NADH regeneration has been shown to efficiently generate labeled products in high isotopic purity (*14*).

NADPH is significantly more expensive than NADH, and currently no widely used system for its regeneration is available. The most promising enzymatic NADPH regeneration system is a mutant FDH from *Pseudomonas* sp. 101 (mut-Pse FDH) available from Jülich Fine Chemicals (Jülich, Germany). However, the enzyme's mutations have not been made public, the catalytic efficiency is low ($1\ \mu M^{-1}\ min^{-1}$), and the cost is high (*16*). Another alternative may be the use of a soluble pyridine nucleotide transhydrogenase which catalyzes the transfer of reducing equivalents between NAD^+ and $NADP^+$ (*17*). Unfortunately, this would require addition of both cofactors and a third enzyme to the process. Currently, the high cost of regenerating enzymes and inefficient regeneration render production processes requiring NADPH not very attractive. It thus became our goal to engineer a mutant PTDH that operates efficiently and with relaxed specificity toward nicotinamide cofactors.

A large body of literature exists describing the alteration of nicotinamide cofactor specificity (*18*−*41*), including two review articles outlining the typical determinants and evolution of nicotinamide binding sites (*42*, *43*). Despite the prevalence of these attempts, altering cofactor specificity remains a challenge, as very few examples exist where catalytic efficiency for the initially disfavored cofactor has been improved to approximate the activity with the preferred substrate (*20*−*28*). Even fewer are the examples where specificity becomes relaxed, allowing high catalytic efficiency with both NAD(H) and NADP(H) (*22*−*25*). Among this last group are the non-Rossman-fold NAD^+-dependent isocitrate dehydrogenase (*22*), glucose−fructose oxidoreductase (*23*), glutathione reductase (*24*), and aldehyde dehydrogenase (*25*). A comparison of the strategies required to achieve efficient use of the nonphysiological cofactor in these enzymes indicates that there is no clear recipe for success.

Rational design was chosen as an initial means to achieve our goal. Unfortunately, the three-dimensional structure of PTDH has not been elucidated yet. However, some information could be gleaned from sequence alignments (Figure 1) and the literature. PTDH contains the consensus sequence of a typical "Rossman"-type fold (*44*, *45*) including the GxxGxGxxG motif common among D-hydroxy acid DHs (Figure 1). Incorporated in this fold is an acidic residue (typically an aspartic acid and in rare cases a glutamic acid), located 18 residues downstream of the glycine motif. In PTDH this position (residue 175) is occupied by the less common glutamic acid (Figure 1). The Asp/Glu residue is thought to provide a significant portion of substrate specificity for NAD(H) by hydrogen bonding to one or both of the 2′- and 3′-hydroxyls of the adenine ribose, whereas NADP(H)-specific dehydrogenases typically have a basic residue nearby this region to interact with the negatively charged 2′-phosphate (*42*, *43*). However, this sequence information alone was not deemed sufficient in lieu of a three-dimensional structure, especially considering that the less common glutamic acid is in the proximity (±13 residues) of three other acidic residues. Therefore, in the present study we describe the construction of a homology model of PTDH. The accuracy of the model was tested by using it as a template to create PTDH mutants with relaxed cofactor specificity. Two single mutants and a double mutant were generated using site-directed mutagenesis, and their kinetics, thermal stabilities, and reaction products are described in this report.

MATERIALS AND METHODS

Materials. Escherichia coli BL21(DE3) and pET15b were purchased from Novagen (Madison, WI). *E. coli* WM1788 and plasmid pLA2 were kindly provided by Professor William Metcalf at the University of Illinois (Urbana, IL) (*46*). The plasmid pRW2 was created from the pLA2 vector by digestion with *Nde*I and *Pci*I to remove the majority of *lac*Z, followed by directional cloning of the PTDH gene digested with the same enzymes. Cloned *PfuTurbo* DNA polymerase was obtained from Stratagene (La Jolla, CA), and *Taq* DNA polymerase was obtained from Promega (Madison, WI). PCR grade dNTPs were obtained from Roche Applied Sciences (Indianapolis, IN). DNA-modifying enzymes *Nde*I, *Pci*I, *Dpn*I, *Bam*HI, and T4 DNA ligase and their corresponding buffers were purchased from New England Biolabs (NEB) (Beverly, MA). D-Glucose was purchased from Fisher Scientific (Pittsburgh, PA), while L-(+)-arabinose and tetrabutylammonium hydrogen sulfate were purchased from Fluka (St. Louis, MO). Ampicillin, kanamycin, isopropyl β-D-thiogalactopyranoside (IPTG), nitro blue tetrazolium (NBT), phenazine methosulfate (PMS), NAD^+, $NADP^+$, NADH, and NADPH were purchased from Sigma (St. Louis, MO). Phosphorous acid was obtained from Aldrich (Milwaukee, WI) and sodium phosphite from Riedel-de Haën (Seelze, Germany). Other required salts and reagents were purchased from either Fisher or Sigma-Aldrich. The QIAprep spin plasmid mini-prep kit, QIAEX II gel purification kit, and QIAquick PCR purification kit were purchased from Qiagen (Valencia, CA). Various oligonucleotide primers were obtained from Integrated DNA Technologies (Coralville, IA). Isoelectric focusing gels (pH 3−9), buffers, SDS−PAGE gels (12%), and protein size markers were purchased from Bio-Rad (Hercules, CA).

Homology Modeling. The following structures were downloaded from the Protein Data Bank (PDB) database (PDB accession code): glycerate dehydrogenase (1GDH) (*47*), phosphoglycerate dehydrogenase (1PSD) (*48*), and D-lactate

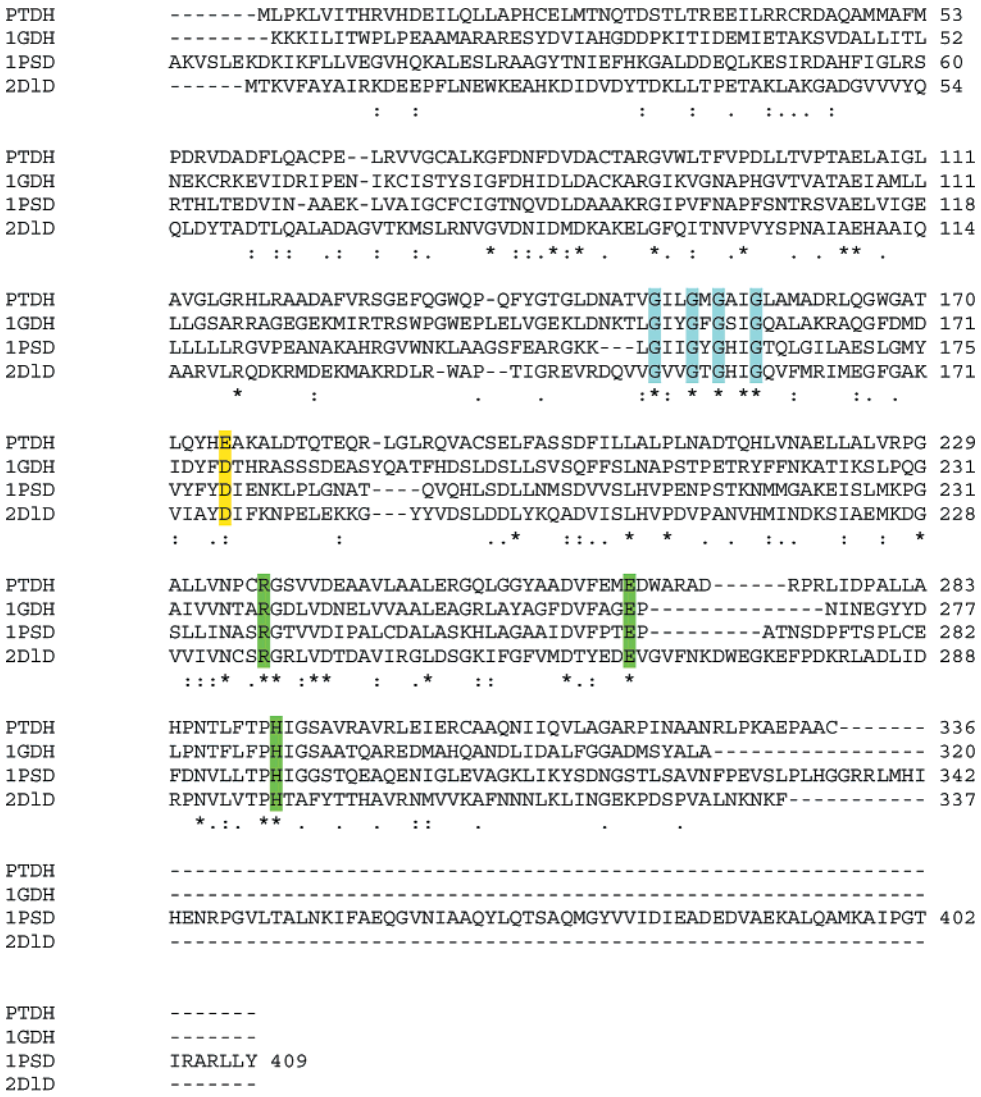

FIGURE 1: Sequence alignment of PTDH with three NAD^+-dependent proteins used for homology modeling including glycerate dehydrogenase (1GDH), phosphoglycerate dehydrogenase (1PSD), and D-lactate dehydrogenase (2DLD). Residues in blue represent the GxxGxGxxG nucleotide binding motif, residues in yellow represent the acidic residue responsible for binding the adenine 2′-hydroxyl group of NAD(H), and residues in green represent the catalytic residues.

dehydrogenase (2DLD). Insight II software (Insight II, version 2000; Accelrys Inc., San Diego, CA) was used to align these three structures by conserved structural regions to achieve the lowest root-mean-square (RMS) score. The amino acid sequence of PTDH was then manually aligned by sequence with the structural alignment, taking great care to make sure that the aligned sequences represented homologous structural regions. This alignment was then used as input for the automated MODELER module within Insight II using default parameters with moderate refinement of the structure and loop regions. Of approximately 30 structural models created, the best model was selected on the basis of visual inspection for obvious flaws, the score from the Profiles 3-D function, and the ProStat inspection of ϕ and ψ angles. NAD^+ from the 2DLD crystal structure was manually docked using the Molecular Operating Environment (MOE; Chemical Computing Group Inc., Montreal, Canada) into the created model, and then the whole structure was subjected to energy minimization to relieve steric and torsional artifacts from the modeling and docking processes. To create mutant enzymes in MOE, a rotamer search was performed with the mutated residue implemented in the homology model of the wild-type (WT) enzyme. The lowest energy conformation was selected and energy minimized with the bound cofactor. All Insight II and MOE calculations were performed in the University of Illinois' School of Chemical Sciences' Computer Application and Network Services (CANS) in the VizLab laboratory.

Site-Directed Mutagenesis. An overlap extension PCR (OE-PCR) method was utilized to introduce site-specific mutations using purified pRW2-PTDH wild type as the template. Two oligonucleotide primers flanking the gene were used in combination with the following mutagenic primers (underlined codons encode desired amino acid substitutions): E175A/G/V forward (5′-CTG CAG TAC CAC GBG GCG AAG GCT CTG-3′, B = T, C, G), E175A/G/V reverse (5′-CAG AGC CTT CGC CVC GTG GTA CTG CAG-3′, V = A, C, G), A176R forward (5′-CAG TAC CAC GAG CGG AAG GCT CTG GAT-3′), A176R reverse (5′-ATC CAG AGC CTT CCG CTC GTG GTA CTG-3′), double mutant forward (5′-CTG CAG TAC CAC GCG CGG AAG GCT CTG GAT AC-3′), double mutant reverse (5′-GT ATC CAT AGC CTT CCG CGC GTG GTA CTG CAG-3′). For the construction of each mutant, two separate PCR

reactions were carried out, each containing one flanking primer and one mutagenic primer. The two PCR products were purified from the agarose gel after DNA electrophoresis, treated with *Dpn*I to remove methylated template, and then elongated by OE-PCR and amplified with the two flanking primers. Products of the correct size were purified from the gel, digested with *Pci*I and *Nde*I, and ligated into the *Pci*I−*Nde*I-digested pRW2 vector. *E. coli* WM1788 was then transformed with the ligation mixture and grown on agar plates containing 50 μg/mL kanamycin. Several colonies were picked, and clones were first analyzed by a cell extract activity assay as described below. Cultures of the clones with desired activity were grown again, and the subsequently isolated plasmids were sequenced in both directions at the Biotechnology Center of the University of Illinois using the BigDye Terminator sequencing method and an ABI PRISM 3700 sequencer (Applied Biosystems, Foster City, CA). The genes containing the desired mutations were then subcloned into the pET15b expression vector as an N-terminal His_6-tag fusion using *Nde*I and *Bam*HI restriction sites. Following subcloning, the mutant genes were again sequenced to eliminate the chance of PCR-introduced random mutations being incorporated into the final DNA construct. The plasmids containing the correct mutant genes were then used to transform *E. coli* BL21(DE3), and colonies selected by ampicillin resistance were used for protein expression and purification.

Cell Extract Activity Assay. A solution of 100 mM Tris-HCl, pH 7.4, with 0.13% (w/v) gelatin and a 10× assay solution consisting of 1 mg/mL NBT, 0.5 mg/mL PMS, 15 mM NAD^+ or 60 mM $NADP^+$, and 40 mM phosphite were prepared. Directly prior to the assay, the latter mixture was diluted 10-fold in the Tris-HCl buffer. Cell lysates from arabinose-induced *E. coli* WM1788 cells containing pRW2-PTDH were prepared by lysozyme incubation and freeze−thaw. Clarified cell extract (50 μL) was aliquoted into a 96-well plate followed by rapid addition of assay mix (150 μL) to each well using a multichannel pipet. The initial rates of reaction and timed end points were observed by measuring the OD_{580} in a Spectramax 340PC microplate reader (Molecular Devices, Sunnyvale, CA).

Overexpression and Purification of PTDH. The buffers used for protein purification included start buffer A (SBA) (0.5 M NaCl, 20% glycerol, and 20 mM Tris-HCl, pH 7.6), start buffer B (SBB) (same as start buffer A but with 10 mM imidazole), and elution buffer (EB) (0.5 M imidazole, 0.5 M NaCl, 20% glycerol, and 20 mM Tris-HCl, pH 7.6). The transformants with pET15b-derived vectors were grown in LB medium containing 100 μg/mL ampicillin at 37 °C with good aeration (shaking at 250 rpm). When the log phase was reached ($OD_{600} \sim 0.6$), cells were induced with IPTG (final concentration 0.3 mM) and incubated at 25 °C with shaking at 250 rpm for 8 h. Cells were harvested by centrifugation at 5000*g*, 4 °C, for 15 min, then resuspended in 3 mL/(g of cell pellet) start buffer A containing 0.6 mg/g of lysozyme, and stored at −80 °C. The frozen cell suspension was thawed at room temperature and lysed by sonication using a Vibra-cell sonicator (Newtown, CT) with amplitude set at 40% and with a pulse sequence of 5 s on and 9.9 s off, for about 8−10 min. Cells were centrifuged at 20000*g* at 4 °C for 10 min, and the supernatant containing the crude extract was filtered through a 0.45 μm filter to remove any particles. The clarified supernatant was purified by FPLC, with a flow rate of 6 mL/min and fraction size of 8 mL. A POROS MC20 column (7.9 mL bed volume) (PerSeptive Biosystems) was charged and equilibrated according to the manufacturer's protocol. The following method was used for purification of PTDH (with His_6 tag) from ∼20−60 mL of clarified supernatant (from ∼5−15 g of cell paste): (1) load sample through pump, 100 mL, (2) wash column with 100 mL of SBB, (3) elute with a linear gradient of 100 mL of 100% SBB to 100% EB in 16.7 min, and (4) wash with 100 mL of EB. The elution fractions were monitored at $\lambda = 280$ nm. PTDH (with His_6 tag) typically eluted from the column halfway through the gradient (40% EB). The protein was concentrated using a Millipore Amicon 8400 stirred ultrafiltration cell with a YM10 membrane at 4 °C, washed twice with 75 mL of 50 mM MOPS buffer (pH 7.25 containing 1 mM DTT and 200 mM NaCl), and concentrated again. The enzyme was then stored as concentrated as possible (usually >2 mg/mL) in 200 μL aliquots at −80 °C in a solution of Amicon wash buffer containing 20% glycerol.

Protein Characterization. Protein concentration was determined by the Bradford method (*49*) using bovine serum albumin as a standard. The purity of the protein was analyzed by SDS−PAGE (*50*). SDS−PAGE gels were stained with Coomassie brilliant blue. The net p*I* of the purified mutants and wild-type proteins was determined by nondenaturing isoelectric focusing (IEF) (*51*). The native IEF gel was subsequently activity stained by the same substrate mixture described above for the cell extract activity assay, allowing visualization of the protein by NBT precipitation.

Kinetic Analysis. Initial rates were determined by monitoring the increase in absorbance, corresponding to the production of NAD(P)H ($\epsilon_{NAD(P)H} = 6.22\ mM^{-1}\ cm^{-1}$ at 340 nm). All initial rate assays were carried out at 25 °C using a Varian Cary 100 Bio UV−visible spectrophotometer. The reaction was initiated by addition of 1.5−3.5 μg of PTDH. Concentrations of NAD^+ stock solutions were determined by UV−visible spectroscopy ($\epsilon_{NAD^+} = 18\ mM^{-1}\ cm^{-1}$ at 260 nm). Phosphite concentrations were determined enzymatically by measuring the amount of NADH produced after all phosphite had been oxidized. Michaelis−Menten constants V_{max} and K_M were determined by a series of assays in which five varying concentrations of one substrate were used in the presence of saturating concentrations (at least 10-fold greater than the corresponding K_M) of the second substrate. The data were then converted to specific activity and fitted with the Michaelis−Menten equation. The WT enzyme and the double mutant were also analyzed by a matrix of 25 assays in which both substrate concentrations were varied from below their K_M to 10-fold above their K_M. These kinetic data were analyzed with a modified version of Cleland's program (*52*). V_{max} and K_M for both phosphite and $NAD(P)^+$ were obtained by fitting the data to a sequential ordered mechanism with $NAD(P)^+$ binding first (*13*):

$$\nu = VAB/(K_{ia}K_B + K_AB + K_BA + AB) \qquad (1)$$

where ν is the initial velocity, V is the maximum velocity, K_A and K_B are the Michaelis−Menten constants for $NAD(P)^+$ and phosphite, respectively, A and B are the concentrations of $NAD(P)^+$ and phosphite, respectively, and K_{ia} is the

Table 1: Kinetic Parameters for Recombinant WT Phosphite Dehydrogenase and Mutants Using $NADP^+$ and NAD^+ as Substrates[a]

	NAD^+				$NADP^+$			
enzyme	K_M (μM, NAD^+)	k_{cat} (min^{-1})	$k_{cat}/K_{M,NAD}$ ($\mu M^{-1}\,min^{-1}$)	K_M (μM, Pt-H)	K_M (μM, $NADP^+$)	k_{cat} (min^{-1})	$k_{cat}/K_{M,NADP}$ ($\mu M^{-1}\,min^{-1}$)	K_M (μM, Pt-H)
WT	53 ± 9.0	175.8 ± 8.4	3.3	47 ± 6.0	2510 ± 410	84.6 ± 0.5	0.0337	1880 ± 325
E175A	16 ± 0.8	210.0 ± 0.3	13.1	23 ± 2.9	144 ± 14	130.8 ± 0.4	0.91	138 ± 25
A176R	60 ± 7.0	256.8 ± 0.5	4.3	156 ± 60	77 ± 8.4	130.8 ± 0.4	1.7	140 ± 20
E175A, A176R	20 ± 1.3	236.4 ± 0.5	11.8	61 ± 13	3.5 ± 0.5	114.0 ± 0.5	32.6	21 ± 2.7

[a] All assays were performed at 25 °C, pH 7.25, in 50 mM MOPS.

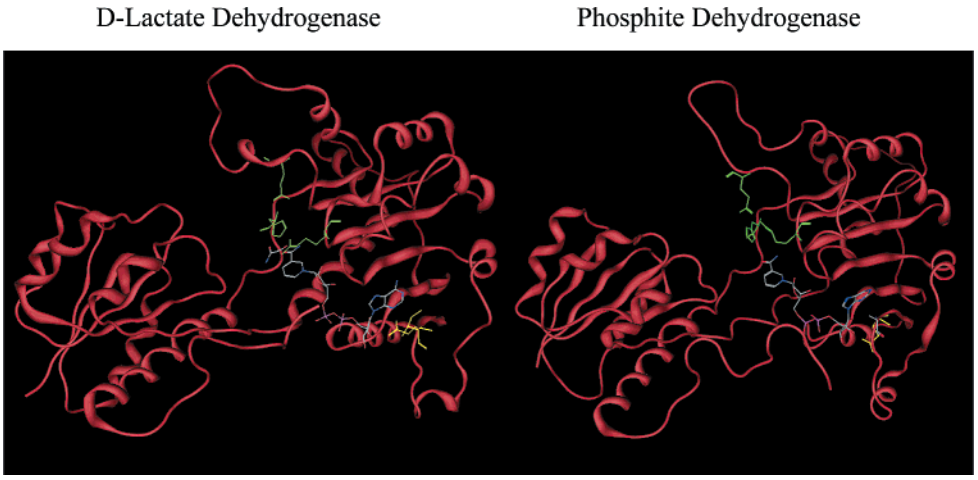

FIGURE 2: Modeled structure of PTDH in comparison to the crystal structure of D-lactate dehydrogenase. The NAD^+ binding domain (Rossman fold) is on the right of each structure, while the catalytic domain is on the left, forming the active site in the middle. Residues in yellow represent the acidic residue responsible for binding the 2′-hydroxyl of NAD(H), and residues in green represent the catalytic residues.

dissociation constant for *A* [$NAD(P)^+$]. All assays were performed in duplicate, and each series of duplicates was performed a minimum of two times. Data presented in Table 1 represent an average of all statistically relevant data.

Thermal Inactivation. Thermal inactivation was studied by incubating either WT or the double mutant at 40.5 °C in 50 mM MOPS (pH 7.25) at a protein concentration of approximately 200 ng/μL. The samples were preincubated on ice for 5 min in the presence of 0.1 mM $NADP^+$, 1 mM $NADP^+$, 1 mM NAD^+, or no cofactor and then placed in the water bath. At various time points 10 μL of the protein sample was used to initiate the reaction of 0.5 mM NAD^+ and 0.5 mM phosphite. Initial activity was measured as described in the Kinetic Analysis section at each time point. The data were plotted as the residual activity versus the incubation time and then analyzed by exponential curve fitting to determine the half-lives of thermal inactivation which followed first-order kinetics.

HPLC Analysis of Reaction Products. The purity of the nicotinamide cofactor substrates and reaction products was assessed by HPLC. The separation of NAD^+, $NADP^+$, NADH, and NADPH was carried out as previously described (*53*) with the following changes. An Agilent 1100 series solvent selector, pump, column, and detector modules were utilized with a Zorbax 150 mm × 3.0 mm C-18 (3.5 μm) column and a flow rate of 0.5 mL/min. Instead of 6 mM tetrabutylammonium phosphate, 5 mM tetrabutylammonium sulfate was used in the mobile phase. The total run time was increased to 20 min by the addition of a 5 min isocratic elution at the end of the gradient. Sample volumes for each pure substrate were 20 μL at a concentration of 1 mM in 50 mM MOPS (pH 7.25). Reaction products were prepared by mixing equal parts of 1 mM $NAD(P)^+$ with 5 mM phosphite, adding approximately 1 μg of enzyme, and allowing the reaction to proceed for 20 min at 30 °C. These samples were then treated the same as authentic samples, tracking the UV absorbance at both 260 nm [λ_{max} $NAD(P)^+$] and 340 nm [λ_{max} NAD(P)H].

RESULTS

Homology Modeling. A protein sequence BLAST search was performed against the Protein Data Bank, and four sequences were chosen from the highest scoring results. They were D-glycerate DH from *Hyphomicrobium methylovorum* (1GDH), D-3-phosphoglycerate DH from *E. coli* (1PSD), D-lactate DH from *Lactobacillus helveticus* (2DLD), and NAD-dependent FDH from *Pseudomonas* sp. 101 (2NAC). These four enzymes represent NAD-specific two-domain D-hydroxy acid dehydrogenases and share between 25% and 30% sequence identity with PTDH. FDH (2NAC) was later excluded from this group as its structure was the most divergent and made the initial structural alignment difficult. The structural model was built as described in Materials and Methods. Once the model was completed, it bore a striking resemblance to D-lactate dehydrogenase as seen in Figure 2, with a RMS difference of 0.55 Å in the polypeptide backbone of the two structures. Using ProStat (Insight II) under default parameters the ϕ and ψ angles were determined to be 79% within their expected values, comparing well to the 74.3%, 80.6%, and 85.8% for the analysis of the template PDB structures 2DLD, 1PSD, and 1GDH, respectively. A value of 90% correct self-compatability of amino acids with the

modeled structure was obtained when inspected by Profiles3-D (Insight II, default parameters).

Three active site residues (Arg237, Glu266, and His292 in PTDH) are highlighted in green in both the sequence alignment (Figure 1) and the structure comparison (Figure 2). The location of these residues in the structure and the sequence is highly conserved in D-hydroxy acid dehydrogenases (*54*). In their typical roles, the histidine acts as an active site base, while the glutamic acid is hydrogen bonded to and raises the pK_a of the histidine, thus making it a stronger base (*54*). The arginine is likely to be involved in binding the typically negatively charged substrates (D-hydroxy acids). It has been previously proposed that these residues, through several possible mechanisms, are involved in catalysis for PTDH (*15*). This is supported by the model showing the close interactions of His292 and Glu266, with Arg237 positioned nearby this dyad. In addition, the hydride-accepting carbon of the modeled NAD$^+$ is very close to these residues (within 5.5 Å of the nearest heavy atom of His292). These observations lend some credibility to the model; however, due to the low sequence homology between PTDH and the three enzymes used as structure templates, it should only be treated as a hypothetical working model until a structure can be obtained by NMR spectroscopy or X-ray crystallography. Accordingly, in our mutant modeling studies as described in the next section, the distance requirement between the donor heteroatom and the acceptor heteroatom of a potential hydrogen bond was relaxed. Although the length of a typical hydrogen bond is 2.6−3.1 Å, a pair of donor and acceptor with a length of 1.6−4.1 Å was considered to be a potential hydrogen bond in our modeling studies.

When different iterations of the modeling output were compared, it was apparent that two regions are highly variable. The first is the loop directly after active site residue Glu266 containing the sequence 267-DWARADRPR-275, and the second is the C-terminal region containing approximately the last 15 residues. The homologous regions for the template dehydrogenases are structurally not well conserved, introducing more freedom in modeling these regions. Furthermore, it is not unusual for loops and termini to obtain several conformations that are nearly equal in energy. The significance of the loop region in this model is that it is involved in the dimerization interface of the protein (in both the model and templates) and is located near the active site. The loop region is fairly well conserved in dehydrogenases that can oxidize phosphite but not in other dehydrogenases (W. W. Metcalf, personal communication). Thus, it is possible that this region containing three arginines is involved in binding phosphite. Another interesting insight was that PTDH ends with Cys336, and it has previously been reported that, for NADP$^+$-dependent malate dehydrogenase, a disulfide bond near the C-terminus helps to regulate enzyme activity by blocking the NADP$^+$ binding site (*55*, *56*). Thus, it is possible that a similar disulfide is formed under certain conditions in PTDH. This hypothesis is supported by the reduced activity when PTDH is purified in the absence of a thiol-reducing reagent such as DTT. Additionally, during the many iterations of homology modeling, the C-terminal region of PTDH was found in many different regional and spatial conformations, most often at or near the NAD$^+$ binding site, further supporting the validity of this hypothesis. The presumed flexibility of the C-terminal region may also be in part responsible for the difficulties experienced during crystallization efforts. These insights from the homology model will be explored in future work.

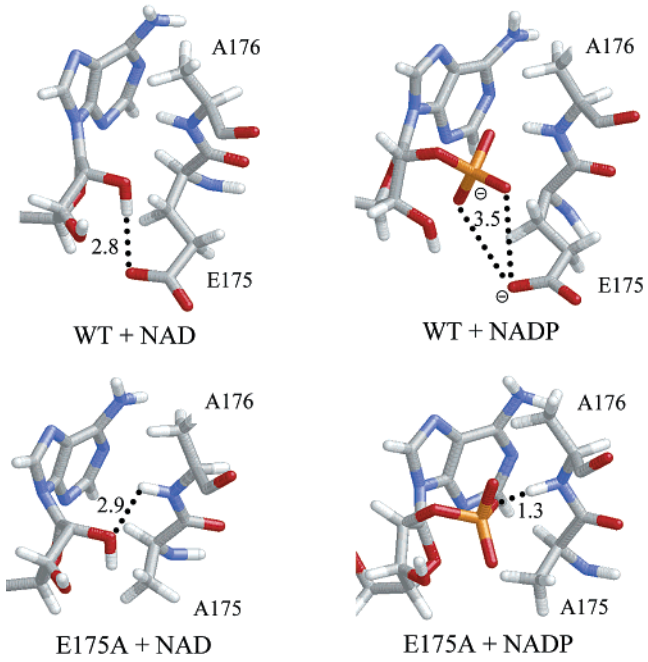

FIGURE 3: Modeled cofactor interactions with mutant enzymes. The interaction between residue E175 of the WT enzyme and the 2′-hydroxyl of NAD$^+$ (the nicotinamide portion is not shown) and the repulsion of this same residue by the 2′-phosphate of NADP$^+$ (the nicotinamide portion is not shown) are apparent. Replacement of this residue with alanine in silico allows both cofactors to form stable interactions with the enzyme. The distances shown are from hydrogen bond acceptor atoms to hydrogen atoms.

Modeling of Mutants with Relaxed Cofactor Specificity. It is apparent from the sequence alignments that PTDH binds NAD$^+$ by a Rossman-type fold, characterized by alternating α/β regions with α-helixes on either side of a plane of six antiparallel β-sheets, and indeed this substructure is present in the model (Figure 2). Among the various hydrogen bond contacts with NAD$^+$ created by the loop regions at the ends of the β-sheets, one particular residue, Glu175, stood out as a possible determinant of cofactor specificity. In the model, this residue may form hydrogen bonds with the hydroxyls of the adenine ribose of NAD$^+$ given their close distance of 2.8 Å (Figure 3), consistent with the sequence alignment prediction (Figure 1). Glu175 would sterically and electrostatically repulse the 2′-phosphate of NADP$^+$, resulting in its poor binding by the WT enzyme. Replacing Glu175 with sterically smaller uncharged residues such as alanine, glycine, and valine was expected to enhance the energetics of NADP$^+$ binding.

The model of a Glu175Ala mutant is shown in Figure 3 in which the phosphate group of NADP$^+$ is not repelled but is allowed to form a possible hydrogen bond with the amide hydrogen of Ala176. This figure also demonstrates that NAD$^+$ can still interact with the Glu175Ala mutant enzyme in a manner similar to that of the WT enzyme with the exceptions of the hydrogen bond contribution from Glu175 and more steric freedom in the mutant binding site. In NADP$^+$-dependent dehydrogenases, a basic residue (most commonly an arginine) involved in binding the 2′-phosphate moiety (*18*, *20*, *21*, *39*−*43*) is typically present at the

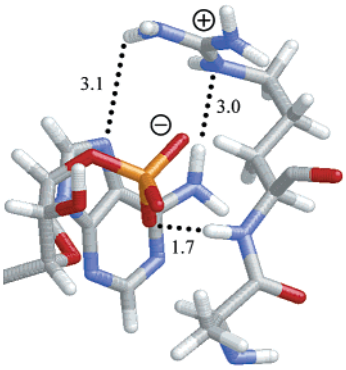

FIGURE 4: A model of the double mutant shows that R176 forms both ionic interactions and H-bonding interactions with $NADP^+$ (the nicotinamide portion is not shown) while A175 allows sufficient room for binding of the 2′-phosphate of $NADP^+$. The distances shown are from hydrogen bond acceptor atoms to hydrogen atoms.

Asp/Glu+1 position. In PTDH, the +1 site is occupied by an alanine (Figure 3). Therefore, the interaction of $NADP^+$ with a double mutant Glu175Ala, Ala176Arg was modeled (Figure 4). In the model, the Arg can engage in electrostatic interactions with the 2′-phosphate of $NADP^+$, while also making hydrogen bond contacts with the adenine base. The model predicts that this mutant would be capable of increasing the catalytic efficiency with $NADP^+$ without significantly reducing the catalytic efficiency with NAD^+.

Mutant Creation, Expression, and Purification. To explore the activity of the modeled mutants, they were first tested with the cell lysate activity assay described in Materials and Methods. Three mutations (Ala, Gly, and Val) at the Glu175 position were generated using mutagenic primers with a single degenerate codon as described in Materials and Methods. Thus, three different gene products were subcloned into the arabinose-inducible pRW2 vector and tested simultaneously. The WM1788 strain of *E. coli* was used in a cell-based assay since it contains a *phoBR* deletion that suppresses activation of endogenous phosphite oxidation pathways in *E. coli* resulting in minimized background activity (*57*). When the lysates of 10 transformed clones expressing Glu175Ala, Glu175Gly, or Glu175Val mutants were assayed with $NADP^+$, four showed significant activity, while the others had activity indistinguishable from background. All 10 clones were subsequently sequenced, revealing that the four active clones contained the Glu175Ala mutation, while Glu175Val and Glu175Gly mutations were both represented in the sequenced DNA from inactive clones. The same pattern was observed in a NAD^+-dependent cell lysate activity assay. This suggests that the Glu175Val and Glu175Gly mutations resulted in inactive proteins, possibly as a result of misfolding, insolubility, or some other type of inactivation. Therefore, Glu175Ala was chosen for additional studies while the other two mutants were not investigated further. Two additional mutants, Ala176Arg and the double mutant Glu175Ala, Ala176Arg, were subsequently generated and assayed. In the cell lysate assay, these two mutants showed a qualitative increase in activity with $NADP^+$ over Glu175Ala and retained high activity with NAD^+ (data not shown).

To further characterize these mutants, they were overexpressed for large-scale purification as His_6-tag fusion proteins. The three mutant genes were inserted into the pET15b expression vector as described in Materials and Methods. Overexpression in *E. coli* BL21(DE3) resulted in production of PTDH at levels greater than 20% of total cellular protein. Ni^{2+} affinity purification resulted in approximately 30−50 mg of highly pure protein from 1.5 L of each culture. SDS−PAGE analysis of the proteins showed no contaminating bands with only the expected 38.5 kDa band from the His_6-tagged monomer (Figure 5A). When the WT protein and the mutant proteins were analyzed on the basis of p*I* by IEF, a clear distinction could be observed (Figure 5B). Both Glu175Ala and Ala176Arg had a more basic p*I* (∼6.2) than the WT protein (∼5.8) due to the removal of the negatively charged residue (Glu175Ala) and the addition of a positively charged residue (Ala176Arg), respectively. The double mutant resulted in a shift toward more basic p*I* (∼6.6), approximately twice as large as for either single mutant when compared to the WT protein (Figure 5B), due to the introduction of a positive residue and the loss of a negative residue. The proteins were activity stained on the basis of NAD^+-dependent PTDH activity, thus clearly showing that all mutants were active with the natural substrate.

Kinetic Analysis. The effect of the mutations on the nicotinamide cofactor preference of PTDH was assessed by comparing the kinetic parameters in the forward reaction (reduction of cofactor). The reverse reaction is too energetically unfavorable to assay by conventional means. The activities of the enzymes were determined as a function of concentration of either cofactor under saturating phosphite concentrations. Then, activities were determined as a function of phosphite concentration in the presence of $NAD(P)^+$ at saturating concentration. For the WT enzyme and the double mutant, a full kinetic assay was used in which both substrate concentrations were varied (Materials and Methods). The results of the kinetic analyses are depicted in Table 1. The turnover number (k_{cat}) of the WT enzyme is slightly lower than previously described due to the assays being performed at 25 °C rather than at 30 °C (*13*) and a slight deactivation by introduction of the His_6 tag. The WT enzyme has a clear preference for NAD^+ over $NADP^+$ by about 100-fold when comparing catalytic efficiency ($k_{cat}/K_{M,NAD(P)}$), primarily as a function of lowered K_M. The effect of the mutations on relaxing this preference by lowering the K_M for $NADP^+$ is obvious. Glu175Ala lowers the K_M by a factor of ∼17, while Ala176Arg lowers the K_M by a factor of ∼33 compared to the WT enzyme. The synergistic effect of these two mutations results in a K_M for $NADP^+$ approximately 700-fold lower in the double mutant. Unexpectedly, the turnover number also improves ∼35−55% in all cases. Therefore, the overall efficiency with $NADP^+$ of the double mutant ($k_{cat}/K_{M,NADP}$) is about 1000-fold higher than that of the WT enzyme. An additional 90-fold improvement in the K_M for phosphite in the presence of $NADP^+$ was observed in the double mutant over the WT enzyme ($K_{M,Pt-H}$ in the presence of NAD^+ remained about the same).

For each mutant enzyme, an improvement in efficiency ($k_{cat}/K_{M,NAD}$) was also obtained with NAD^+ as the substrate. The K_M for NAD^+ was reduced for both Glu175Ala and the double mutant while it was similar to WT for Ala176Arg, suggesting that the Glu175Ala mutation was responsible for reducing the K_M in the double mutant. It is not clear from

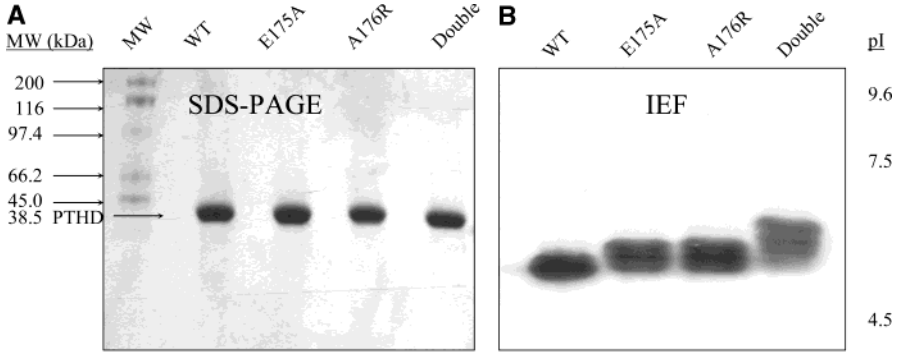

FIGURE 5: (A) SDS−PAGE analysis of the purified WT and mutant PTDH proteins. (B) Isoelectric focusing native gel analysis of the same protein samples. The proteins are separated on the basis of p*I*, showing that both single mutants have a higher p*I* as predicted and that the effect is additive for the double mutant.

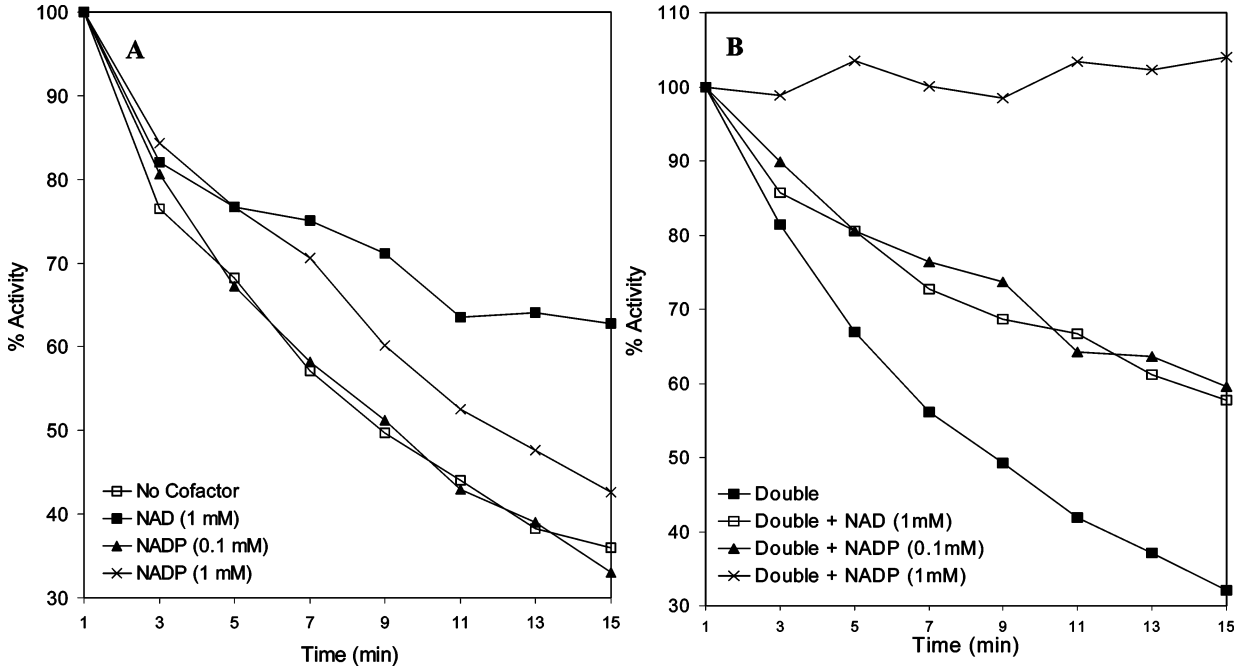

FIGURE 6: Thermal inactivation of WT and the double mutant PTDH at 40.5 °C. (A) WT PTDH is inactivated with a half-life of 9.6 min, but in the presence of 1 mM NAD^+ (and not 0.1 mM or 1 mM $NADP^+$), it forms a more thermally stable enzyme−substrate complex with a half-life of 23 min. (B) The double mutant PTDH is inactivated with a half-life of 8.8 min. In the presence of both 1 mM NAD^+ and 0.1 mM $NADP^+$ the double mutant forms a thermally stable enzyme substrate complex with half-lives around 19 min. In the presence of 1 mM $NADP^+$ the double mutant retains approximately 100% activity over the 15 min period.

the modeling alone why Glu175Ala has a lower K_M for NAD^+ than the wild-type enzyme, although the models in Figure 3 suggest that the backbone amide of Ala176 may form a hydrogen bond that can compensate for the loss of the hydrogen bond formed between the 2′-hydroxyl group of NAD^+ and the carboxyl group of Glu175Ala. The turnover number was improved as well, with the highest increase of nearly 46% for Ala176Arg. The increase in k_{cat} for the double mutant of about 34% coupled with the reduction in K_M for NAD^+ (2.7-fold) resulted in an approximate 3.6-fold increase in catalytic efficiency ($k_{cat}/K_{M,NAD}$).

HPLC Analysis of Reaction Products. The purity of the nicotinamide substrates was analyzed to verify that the observed activity was not the result of contamination. Samples of the oxidized cofactors $NAD(P)^+$ were therefore prepared (Sigma) and analyzed by ion-pair HPLC. There was no discernible NAD^+ present in the $NADP^+$ sample, which appeared to be greater than 99% pure (data not shown). When analyzing NAD^+, a small amount (∼2%) of $NADP^+$ was present (data not shown). To verify that NADPH was the respective product of $NADP^+$ reduction by the PTDH double mutant, a small-scale reaction was carried out. When the products were analyzed by HPLC, a single peak (UV 340 nm) was observed that had the same retention time as authentic NADPH. The same process was carried out for NAD^+ as the substrate, and again a peak was observed with a retention time corresponding to an authentic sample of NADH. A small peak with the retention time of NADPH was also observed, corresponding to the reduction of the small amount (∼2%) of $NADP^+$ present in the NAD^+ starting material, providing an internal control.

Thermal Stability and $NAD(P)^+$ Protection. WT PTDH proved relatively stable at 25 °C (data not shown); however, at higher temperatures, irreversible thermal inactivation was observed. The WT enzyme gradually lost its activity over a 15 min period at 40.5 °C (Figure 6A) with a half-life ($t_{1/2}$) of 9.6 min. The thermal stability of the double mutant was very similar, with a $t_{1/2}$ of 8.8 min (Figure 6B). Preincubation

of the WT enzyme with 1 mM NAD^+ protected the enzyme from inactivation, lengthening the $t_{1/2}$ to nearly 23 min, while preincubation with 1 mM $NADP^+$ afforded almost no protection ($t_{1/2} = 11.1$ min) (Figure 6A). Performing the same experiment with the double mutant resulted in retention of 100% activity for 15 min in the presence of 1 mM $NADP^+$ and thus complete protection from thermal inactivation over that short time period. In the presence of 1 mM NAD^+, protection was similar to that of WT ($t_{1/2} = 18.9$ min) (Figure 6B). Furthermore, when the $NADP^+$ concentrations were reduced to 0.1 mM, the WT enzyme was not protected ($t_{1/2} = 9.1$ min), while the double mutant was still significantly protected with $t_{1/2} = 19.1$ min. This provides further support that the WT enzyme has a higher affinity for NAD^+ than for $NADP^+$, while the double mutant has relaxed cofactor specificity and strongly binds $NADP^+$ and NAD^+.

DISCUSSION

In this study we have shown that by site-directed mutagenesis of two residues, Glu175 and Ala176, the nicotinamide cofactor specificity of PTDH was relaxed while the enzyme activity with both cofactors was enhanced. This suggests that the charged residues near the 2′-position of NAD^+ are responsible for cofactor selectivity as previously described (*18*, *20*, *21*, *39*−*43*). However, our result is different from most studies of this type where activity with one or both cofactors is reduced in order to achieve a specificity change (*18*−*21*, *26*−*31*, *33*−*41*). In very few instances high catalytic efficiency accompanies the relaxation of specificity for NAD(H) and NADP(H) (*22*−*25*). These examples include an increased activity with both cofactors for the non Rossman-fold NAD^+-dependent isocitrate dehydrogenase by the mutation of Asp328 to Lys (*22*), enhanced activity with both cofactors for glutathione reductase by deleting a loop near the cofactor binding domain (*24*), changing the catalytic activity of glucose−fructose oxidoreductase to that of a dehydrogenase as well as increasing cofactor promiscuity by various combinations of five mutations (*23*), and increasing the catalytic efficiency with both substrates in aldehyde dehydrogenase via a single mutation of Thr175 to Gln (*25*). In all of these cases (*22*−*25*) either many mutations and combinations were attempted or extensive knowledge of the enzyme structure and homologous structures with opposite specificity was available.

The primary effect of the mutations in PTDH was on the Michaelis constants (K_M) of PTDH for $NADP^+$ and phosphite (in the presence of $NADP^+$), while smaller effects were seen in k_{cat} with both NAD^+ and $NADP^+$ as substrates. Previously, the activity of WT PTDH with 1 mM phosphite and 6 mM $NADP^+$ was estimated to be about 7% compared to the activity with 1 mM NAD^+ and 1 mM phosphite (*13*). However, we found here that the k_{cat} with $NADP^+$ is nearly 50% of the k_{cat} with NAD^+. The reason for this discrepancy is that the concentration of phosphite previously used was well below its K_M (in the presence of $NADP^+$). The K_M was not determined for either substrate ($NADP^+$ or phosphite) as the reaction with $NADP^+$ was not the focus of the previous study (*13*).

Replacing Ala176 with a positively charged residue (Arg) had the largest effect on the K_M of $NADP^+$, but replacing the large negatively charged residue (Glu) with alanine also had a pronounced effect. The synergistic effect of these two mutations was larger than the effect of the two individual mutations. The resulting double mutant uses $NADP^+$ with 1000-fold greater efficiency ($k_{cat}/K_{M,NADP}$) and NAD^+ with 3.6-fold greater efficiency ($k_{cat}/K_{M,NAD}$) than WT. When comparing catalytic efficiency, the specificity for the cofactor changes from about 100-fold in favor of NAD^+ for the WT enzyme to about 3-fold in favor of $NADP^+$ for the double mutant. With all mutants and for both cofactors the turnover number (k_{cat}) was higher than for WT. An increase in the catalytic efficiency upon mutagenesis without adverse effect in some other property such as k_{cat} or K_M for the second substrate is a relatively rare observation.

The ultimate purpose for the mutant enzymes is their use in cofactor regeneration, and therefore, a decrease in thermal stability is undesired. The $t_{1/2}$ of thermal inactivation at 40.5 °C was determined for the WT enzyme and the double mutant. Since the half-lives are nearly identical (9.6 and 8.8 min, respectively), the mutations have no significant effect on thermal stability. It has been previously shown that when dehydrogenases bind their nicotinamide cofactor, they form a thermally more stable enzyme−substrate complex, but little to no effect is seen when the cofactor remains unbound (*25*, *33*). From the results of thermal inactivation in the presence of either cofactor, it is clear that the WT PTDH forms a complex only with NAD^+, whereas the double mutant forms a complex with both NAD^+ and $NADP^+$. This provides further evidence that the increase in activity with $NADP^+$ is due mostly to enhanced binding of $NADP^+$ to the enzyme without disrupting the binding of NAD^+.

Since NAD^+ and $NADP^+$ differ only by a 2′-phosphate group, it was possible that the mutant enzyme dephosphorylated $NADP^+$ to NAD^+ and the observed activity was due to reduction of NAD^+. It was also possible that some NAD^+ was present in the $NADP^+$ used in the experiments, which would complicate the results. Therefore, HPLC was used to analyze the starting materials and enzymatic products. No NAD^+ was present in the $NADP^+$ samples within the detection limits of HPLC; however, the reverse was not true. The slight contamination of $NADP^+$ in the NAD^+ was not a problem since the enzymes all utilized NAD^+ with low K_M's and the contamination level was only ∼2%. When examining the reaction products, NADPH was produced from $NADP^+$ and NADH from NAD^+. Further examination of the HPLC data indicated no detectable remaining oxidized cofactor after reaction. This clearly shows that the reaction proceeds essentially to completion under physiological conditions and can provide a potent driving force when coupled to unfavorable reactions.

As mentioned in the introduction, the currently most useful enzyme for $NADP^+$ regeneration is a mutant *Pseudomonas* sp. 101 FDH (mut-Pse FDH) available from Jülich Fine Chemicals (*16*). The PTDH double mutant described here has a catalytic efficiency with $NADP^+$ ($k_{cat}/K_{M,NADP}$) that is about 33-fold higher than that of mut-Pse FDH with comparable turnover numbers of 114 and 150 min^{-1}, respectively (*16*, *39*). Moreover, the PTDH double mutant can regenerate both cofactors and has a catalytic efficiency with NAD^+ ($k_{cat}/K_{M,NAD}$) that is 39-fold greater than mut-Pse FDH, again with comparable turnover numbers of 236.4 and 300 min^{-1}, respectively. In fact, its catalytic efficiency with NAD^+ even slightly exceeds (∼18%) that of WT Pse

FDH (*16*, *39*). Additionally, whereas the FDH mutants were assayed near optimal conditions (30 °C), PTDH mutants were assayed at 25 °C. The k_{cat} of WT PTDH is reduced at 25 °C in comparison to its activity at 35 °C (*13*), and hence the improvement over mut-Pse FDH is underestimated. Finally, an approximately 100-fold lower concentration of the second substrate (phosphite versus formate) is required for maximal activity with PTDH than with mut-Pse FDH. From this vantage point, the PTDH double mutant represents a very promising NADPH regeneration system.

The relaxation of cofactor specificity described here was achieved by protein engineering based largely on structural information derived from homology modeling and sequence similarity with other $NAD(P)^+$-dependent dehydrogenases. From the homology model, it was predicted that the double mutant should bind $NADP^+$ by electrostatic and hydrogen bond interactions between Arg176 and the cofactor, while Ala175 would not interfere with its binding (Figure 4). The success of this strategy suggests that the homology model is at least a good working hypothesis for the structure of PTDH. Algorithms that align sequences and create model structures are powerful mathematical tools that in this case made it possible to perform rational design. However, these methods are based on assumptions, including how much we understand protein structure−function relationships and protein folding. Therefore, the structural model should be used cautiously.

Future characterization of the PTDH double mutant will include performance in small-scale reactor settings for actual cofactor regeneration in synthetic reactions. Furthermore, rational design involving the PTDH-specific loop region discussed above may provide better insight into what allows PTDH to catalyze this energetically "easy" reaction while other related DHs cannot. Currently, directed molecular evolution of PTDH for higher turnover number (k_{cat}) with $NAD(P)^+$ is being investigated. The random mutations incorporated in selected mutants and their position in the homology model should aid in understanding catalysis and enable reaching the ultimate goal of developing the enzyme into a highly efficient, low cost, multiple nicotinamide cofactor regeneration biocatalyst.

ACKNOWLEDGMENT

We thank Professor Metcalf for providing us with the pLA2 plasmid and the screening strain *E. coli* WM1788 and for helpful conversations. We also thank the School of Chemical Sciences' CANS group for help in the calculations and for access to MOE and Insight II software.

REFERENCES

1. Zaks, A. (2001) *Curr. Opin. Chem. Biol. 5*, 130−136.
2. Schmid, A., Dordick, J. S., Hauer, B., Kiener, A., Wubbolts, M., and Witholt, B. (2001) *Nature 409*, 258−268.
3. Liese, A., and Filho, M. V. (1999) *Curr. Opin. Biotechnol. 10*, 595−603.
4. Koeller, K. M., and Wong, C. H. (2001) *Nature 409*, 232−240.
5. Zhao, H., Chockalingam, K., and Chen, Z. (2002) *Curr. Opin. Biotechnol. 13*, 104−110.
6. Faber, K. (1997) in *Biotransformations In Organic Chemistry: A Textbook*, 3rd ed., Springer-Verlag, Berlin, Germany.
7. Berrios-Rivera, S. J., Bennett, G. N., and San, K. Y. (2002) *Metab. Eng. 4*, 217−229.
8. Leonida, M. D. (2001) *Curr. Med. Chem. 8*, 345−369.
9. Chenault, H. K., and Whitesides, G. M. (1987) *Appl. Biochem. Biotechnol. 14*, 147−197.
10. van der Donk, W. A., and Zhao, H. (2003) *Curr. Opin. Biotechnol. 14*, 421−426.
11. Bommarius, A. S., and Drauz, K. (1994) *Bioorg. Med. Chem. 2*, 617−626.
12. McCoy, M. (2001) *Chem. Eng. News 79*, 37−43.
13. Costas, A. M., White, A. K., and Metcalf, W. W. (2001) *J. Biol. Chem. 276*, 17429−17436.
14. Vrtis, J. M., White, A., Metcalf, W. W., and van der Donk, W. A. (2002) *Angew. Chem., Int. Ed. Engl. 41*, 3257−3259.
15. Vrtis, J. M., White, A. K., Metcalf, W. W., and van der Donk, W. A. (2001) *J. Am. Chem. Soc. 123*, 2672−2673.
16. Tishkov, V. I., Galkin, A. G., Fedorchuk, V. V., Savitsky, P. A., Rojkova, A. M., Gieren, H., and Kula, M. R. (1999) *Biotechnol. Bioeng. 64*, 187−193.
17. Boonstra, B., Rathbone, D. A., French, C. E., Walker, E. H., and Bruce, N. C. (2000) *Appl. Environ. Microbiol. 66*, 5161−5166.
18. Scrutton, N. S., Berry, A., and Perham, R. N. (1990) *Nature 343*, 38−43.
19. Feeney, R., Clarke, A. R., and Holbrook, J. J. (1990) *Biochem. Biophys. Res. Commun. 166*, 667−672.
20. Bocanegra, J. A., Scrutton, N. S., and Perham, R. N. (1993) *Biochemistry 32*, 2737−2740.
21. Nishiyama, M., Birktoft, J. J., and Beppu, T. (1993) *J. Biol. Chem. 268*, 4656−4660.
22. Steen, I. H., Lien, T., Madsen, M. S., and Birkeland, N. K. (2002) *Arch. Microbiol. 178*, 297−300.
23. Wiegert, T., Sahm, H., and Sprenger, G. A. (1997) *J. Biol. Chem. 272*, 13126−13133.
24. Danielson, U. H., Jiang, F., Hansson, L. O., and Mannervik, B. (1999) *Biochemistry 38*, 9254−9263.
25. Zhang, L., Ahvazi, B., Szittner, R., Vrielink, A., and Meighen, E. (1999) *Biochemistry 38*, 11440−11447.
26. Nakanishi, M., Matsuura, K., Kaibe, H., Tanaka, N., Nonaka, T., Mitsui, Y., and Hara, A. (1997) *J. Biol. Chem. 272*, 2218−2222.
27. Galkin, A., Kulakova, L., Ohshima, T., Esaki, N., and Soda, K. (1997) *Protein Eng. 10*, 687−690.
28. Schepens, I., Johansson, K., Decottignies, P., Gillibert, M., Hirasawa, M., Knaff, D. B., and Miginiac-Maslow, M. (2000) *J. Biol. Chem. 275*, 20996−21001.
29. Banta, S., and Anderson, S. (2002) *J. Mol. Evol. 55*, 623−631.
30. Banta, S., Swanson, B. A., Wu, S., Jarnagin, A., and Anderson, S. (2002) *Biochemistry 41*, 6226−6236.
31. Chen, R., Greer, A., and Dean, A. M. (1995) *Proc. Natl. Acad. Sci. U.S.A. 92*, 11666−11670.
32. Chen, R., Greer, A., and Dean, A. M. (1996) *Proc. Natl. Acad. Sci. U.S.A. 93*, 12171−12176.
33. Corbier, C., Clermont, S., Billard, P., Skarzynski, T., Branlant, C., Wonacott, A., and Branlant, G. (1990) *Biochemistry 29*, 7101−7106.
34. Grimshaw, C. E., Matthews, D. A., Varughese, K. I., Skinner, M., Xuong, N. H., Bray, T., Hoch, J., and Whiteley, J. M. (1992) *J. Biol. Chem. 267*, 15334−15339.
35. Holmberg, N., Ryde, U., and Bulow, L. (1999) *Protein Eng. 12*, 851−856.
36. Huang, Y. W., Pineau, I., Chang, H. J., Azzi, A., Bellemare, V., Laberge, S., and Lin, S. X. (2001) *Mol. Endocrinol. 15*, 2010−2020.
37. Hurley, J. H., Chen, R., and Dean, A. M. (1996) *Biochemistry 35*, 5670−5678.
38. Lauvergeat, V., Kennedy, K., Feuillet, C., McKie, J. H., Gorrichon, L., Baltas, M., Boudet, A. M., Grima-Pettenati, J., and Douglas, K. T. (1995) *Biochemistry 34*, 12426−12434.
39. Serov, A. E., Popova, A. S., Fedorchuk, V. V., and Tishkov, V. I. (2002) *Biochem. J. 367*, 841−847.
40. Wang, H., Lei, B., and Tu, S. C. (2000) *Biochemistry 39*, 7813−7819.
41. Yaoi, T., Miyazaki, K., Oshima, T., Komukai, Y., and Go, M. (1996) *J. Biochem. 119*, 1014−1018.
42. Carugo, O., and Argos, P. (1997) *Proteins 28*, 10−28.
43. Carugo, O., and Argos, P. (1997) *Proteins 28*, 29−40.
44. Rossmann, M. G., Moras, D., and Olsen, K. W. (1974) *Nature 250*, 194−199.
45. Wierenga, R. K., De Maeyer, M. C. H., and Hol, W. G. J. (1985) *Biochemistry 24*, 1346−1357.
46. Haldimann, A., and Wanner, B. L. (2001) *J. Bacteriol. 183*, 6384−6393.

47. Goldberg, J. D., Yoshida, T., and Brick, P. (1994) *J. Mol. Biol. 236*, 1123−1140.
48. Schuller, D. J., Grant, G. A., and Banaszak, L. J. (1995) *Nat. Struct. Biol. 2*, 69−76.
49. Bradford, M. M. (1976) *Anal. Biochem. 72*, 248−254.
50. Laemmli, U. K. (1970) *Nature 227*, 680−685.
51. Hara, A., Deyashiki, Y., Nakagawa, M., Nakayama, T., and Sawada, H. (1982) *J. Biochem. 92*, 1753−1762.
52. Cleland, W. W. (1979) *Methods Enzymol. 63*, 103−138.
53. Micheli, V., Simmonds, H. A., Bari, M., and Pompucci, G. (1993) *Clin. Chim. Acta 220*, 1−17.
54. Kochhar, S., Lamzin, V. S., Razeto, A., Delley, M., Hottinger, H., and Germond, J. E. (2000) *Eur. J. Biochem. 267*, 1633−1639.
55. Issakidis, E., Saarinen, M., Decottignies, P., Jacquot, J. P., Cretin, C., Gadal, P., and Miginiac-Maslow, M. (1994) *J. Biol. Chem. 269*, 3511−3517.
56. Krimm, I., Goyer, A., Issakidis-Bourguet, E., Miginiac-Maslow, M., and Lancelin, J. M. (1999) *J. Biol. Chem. 274*, 34539−34542.
57. Metcalf, W. W., and Wanner, B. L. (1991) *J. Bacteriol. 173*, 587−600.

BI035018B